Tanvi Singh

Thesis M.Sc Prerna

Technical Paper Plag Check

Document Details

Submission ID
trn:oid:::27535:143624943

Submission Date
Jun 19, 2026, 1:53 PM GMT+5:30

Download Date
Jun 19, 2026, 3:06 PM GMT+5:30

File Name
Thesis M.Sc Prerna.docx

File Size
2.8 MB

53 Pages

8,614 Words

48,726 Characters

5% Overall Similarity

The combined total of all matches, including overlapping sources, for each database.

Filtered from the Report

- Bibliography
- Quoted Text
- Cited Text
- Small Matches (less than 10 words)

Exclusions

- 10 Excluded Matches

Match Groups

6 Not Cited or Quoted 5%
Matches with neither in-text citation nor quotation marks

0 Missing Quotations 0%
Matches that are still very similar to source material

0 Missing Citation 0%
Matches that have quotation marks, but no in-text citation

0 Cited and Quoted 0%
Matches with in-text citation present, but no quotation marks

Top Sources

2% Internet sources
2% Publications
5% Submitted works (Student Papers)

Integrity Flags

0 Integrity Flags for Review

Our system's algorithms look deeply at a document for any inconsistencies that would set it apart from a normal submission. If we notice something strange, we flag it for you to review.

A Flag is not necessarily an indicator of a problem. However, we'd recommend you focus your attention there for further review.

Match Groups

- **6** Not Cited or Quoted 5%
  Matches with neither in-text citation nor quotation marks
- **0** Missing Quotations 0%
  Matches that are still very similar to source material
- **0** Missing Citation 0%
  Matches that have quotation marks, but no in-text citation
- **0** Cited and Quoted 0%
  Matches with in-text citation present, but no quotation marks

Top Sources

2% Internet sources
2% Publications
5% Submitted works (Student Papers)

Top Sources

The sources with the highest number of matches within the submission. Overlapping sources will not be displayed.

1	Internet	
pure.kfupm.edu.sa		1%
2	Student papers	
Delhi Technological University on 2026-06-10		<1%
3	Student papers	
Pakistan Institute of Engineering & Applied Sciences, Islamabad (PIEAS) on 2026-0...		<1%
4	Student papers	
Delhi Technological University on 2026-04-09		<1%
5	Publication	
Achraf Berradi, Ahlam Lafdali, Naaila Ouazzani, Khalid Aziz et al. "Development a...		<1%
6	Student papers	
Delhi Technological University on 2026-05-21		<1%

Superabsorbent *Prunus domestica* and Tannin Grafted Hydrogel with Extended Release of Pesticide Dinotefuran for Agricultural Application

A DISSERTATION

SUBMITTED IN PARTIAL FULFILLMENT OF THE REQUIREMENTS
FOR THE AWARD OF THE DEGREE

OF

MASTERS OF SCIENCE

IN

CHEMISTRY

Submitted by

Prerna Gupta

(24/MSCCHE/18)

Under the Supervision of
Prof. R. K. Gupta & Prof. D. Kumar

DEPARTMENT OF APPLIED CHEMISTRY

DELHI TECHNOLOGICAL UNIVERSITY
(Formerly Delhi College of Engineering)
Shahbad Daulatpur Bawana Road, Delhi -110042
JUNE, 2026

DELHI TECHNOLOGICAL UNIVERSITY
(Formerly Delhi College of Engineering)
Shahbad Daulatpur, Main Bawana Road,
Delhi -110042

CANDIDATE'S DECLARATION

I, Prerna Gupta (24/MSCCHE/18), declare that the work reported in the dissertation entitled "**Superabsorbent *Prunus domestica* and Tannin Grafted Hydrogel with Extended Release of Pesticide Dinotefuran for Agricultural Application**" submitted in partial fulfilment of the requirement for award of the Degree of Master of Science in Chemistry to the department of Applied Chemistry, Delhi Technological University, Delhi, for the academic session 2025-2026 is an record of our own research work carried out during the period of study (2025-2026) under the supervision of Prof. R. K. Gupta and Prof. D. Kumar.

The matter presented in the thesis has not been submitted by us for the award of any other degree of this or any other Institute.

Place: Delhi **Prerna Gupta**

Date: **(24/MSCCHE/18)**

Department of Applied Chemistry
DELHI TECHNOLOGICAL UNIVERSITY
(Formerly Delhi College of Engineering)
Shahbad Daulatpur, Main Bawana Road, Delhi -110042

CERTIFICATE

It is certified that Prerna Gupta (24/MSCCHE/18) has done their project work as disclosed in this thesis entitled **"Superabsorbent *Prunus domestica* and Tannin Grafted Hydrogel with Extended Release of Pesticide Dinotefuran for Agricultural Application"** for the partial fulfilment of their degree of Master of Science in Chemistry by Department of Applied Chemistry, Delhi Technological University, Delhi, under my guidance. The dissertation reflects the results of original work, and studies are conducted by the students themselves, and the content of the thesis does not serve as the foundation for awarding any other degree to the candidate or any other body from this or any other University/Institution.

Place: Delhi
Date:

Prof. R. K. Gupta & Prof. D. Kumar
(Supervisor)

DELHI TECHNOLOGICAL UNIVERSITY
(Formerly Delhi College of Engineering)
Shahbad Daulatpur, Main Bawana Road, Delhi -110042

ACKNOWLEDGEMENT

I would like to express my deepest gratitude to my supervisors, Prof. R. K. Gupta & Prof. D. Kumar, Department of Applied Chemistry, Delhi Technological University, Delhi. Their consistent guidance, invaluable suggestions, and ongoing encouragement have helped me to complete this work. It has been a privilege to work under such a kind, motivated, and supportive mentors.

I was fortunate to experience a positive work environment in the laboratory and grateful to all the laboratory staff and research scholars for their cooperation. I am particularly thankful to Ms. Vaishali Prashar (PhD scholar) for her extensive help in teaching me the fundamentals of techniques and for her patience in addressing my numerous questions throughout my research. I am also thankful to Ms. Tanvi and Ms. Nishtha for their support of our project. I am deeply appreciative of all the faculty members of the Department of Applied Chemistry at DTU for their ongoing support and cooperation. Additionally, I extend our thanks to both the technical and non-technical staff for their assistance whenever it was needed.

Finally, I want to express my heartfelt gratitude to my family and friends, especially Mamata Singh, Varsha Sheoran, Vinay Rastogi, and Aaditya, for their encouragement, support, and motivation throughout this journey.

Prerna Gupta

ABSTRACT

The development of sustainable agricultural systems requires innovative and environmentally friendly materials which effectively address huge challenges such as water shortage, extensive pesticide usage, and decrease in productivity of crops. In the present era, polymer-based delivery carriers have emerged as an excellent tool because of their high capacities to absorb water, controlled release behaviour and biodegradability. In the present study, natural polymers derived from gum of *Prunus domestica* and Tannin from *Acacia catechu* have been employed to prepared grafted hydrogels intended for agricultural applications. The individual hydrogels, namely PD-g-SAH and AC-g-SAH, along with the combined hydrogel system PDAC-g-SAH, were synthesized through a free-radical copolymerization process using N,N′-methylenebisacrylamide (N,N MBA) as the crosslinker. Naturally derived components were incorporated to maintain sustainability.

A comparative study of the synthesized hydrogel formulations was performed to test their swelling index, water retention capacity (WRC) and release duration in distilled water. Among the synthesised hydrogels, the combination was proven to be superior with respect to individual hydrogels in terms of swelling index, water retention capacity (WRC) and release study, indicating its potential to maintain soil hydration over extended periods. Such properties are highly useful in agricultural fields where effective water management is essential for plant growth and productivity, especially in drought-prone areas.

Grafting process, thermal behaviour, strength and surface morphology were confirmed using the characterization techniques. Fourier-transform infrared spectroscopy (FT-IR) and ^{13}C nuclear magnetic resonance (^{13}C NMR) analyses verified the presence of functional groups and successful copolymerization within the hydrogel matrix. X-ray diffraction (XRD) studies revealed the structural arrangement and degree of crystallinity, while scanning electron microscopy (SEM) provided information regarding the porous surface morphology responsible for

enhanced swelling and pesticide encapsulation. Thermogravimetric analysis (TGA) demonstrated the thermal stability of the synthesized materials, and rheological investigations confirmed their mechanical strength and viscoelastic properties, which are important for practical agricultural applications.

The prepared hydrogels were further evaluated as controlled-release carriers for the pesticide dinotefuran. The pesticide loading efficiencies after 48 hours were recorded as 54.97% for PDAC-g-SAH, 47.27% for PD-g-SAH, and 31.49% for AC-g-SAH, indicating that the combined hydrogel possessed the highest loading capacity due to its improved network structure and porosity. Release studies showed that the dinotefuran was released gradually and continuously from the hydrogel matrices over time, minimizing the sudden release of pesticide into the environment. The release kinetics were best explained by Korsmeyer–Peppas, Higuchi, and first-order kinetic models, suggesting that diffusion-controlled mechanisms played a significant role in pesticide release.

The extended-release behaviour of the PDAC-g-SAH hydrogel highlights its capability in reducing pesticide loss caused by leaching, runoff, and evaporation. This not only improves the persistence and utilization efficiency of dinotefuran but also lowers the frequency of pesticide application, thereby reducing environmental contamination and economic costs for farmers. Overall, the study demonstrates that the developed natural polymer-based hydrogel system represents a promising and eco-friendly strategy for water conservation and controlled pesticide delivery, supporting the advancement of sustainable and efficient agricultural practices.

Contents

Declaration II

Certificate III

Acknowledgement IV

Abstract V

Contents VII

List of Figures IX

List of Tables X

List of Abbreviations XI

CHAPTER 1: INTRODUCTION AND LITERATURE REVIEW

1. Introduction 1-5

CHAPTER 2: MATERIAL AND METHODOLOGY

2.1 Materials 6

2.2 Synthesis 6

2.3 Swelling studies of the synthesised hydrogels 6-7

2.4 Characterization 7

2.5 Water Retention Capacity (WRC) 7-8

2.6 Encapsulation and release study of dinotefuran using PDAC-g-SAH, PD- g-SAH, and AC-g-SAH 8-9

2.6.1 Percentage Loading

CHAPTER 3: SPECIFICATIONS OF *PRUNUS DOMESTICA* AND TANNIN

3.1 Specifications of *Prunus Domestica* 10-11

3.2 Specifications of Tannin 12-13

6

CHAPTER 4: RESULTS AND DISCUSSION

4.1 Reaction Mechanism	14-16
4.2 Swelling study	16-19
4.2.1 Effect of concentration of biopolymer on SI	
4.2.2 Variation of SI with respect to time	
4.3Physical features of the synthesized hydrogel	19
4.4 Characterization	20-25
4.4.1 FT-IR	
4.4.2 ^{13}C NMR	
4.4.3 XRD	
4.4.4 SEM	
4.4.5 TGA	
4.4.6 Rheology	
4.5 Water Retention Capacity	26
4.6 Encapsulation of dinotefuran and release kinetics	26-29
4.6.1 Percentage Loading	
4.6.2 Release Kinetics	
CHAPTER 5: CONCLUSION AND FUTURE PROSPECTS	30-31
Journal Publication	
References	32-39

LIST OF FIGURES

Fig. 1 Structure for Catechin and Epicatechin

Fig. 2 Structure for condensed tannins

Fig. 3 Raw image of PD gum

Fig. 4 Chemical structure of dinotefuran

Fig. 5 Powdered PD gum

Fig. 6 Powdered form of tannin

Fig. 7 Mechanistic pathway of formation of PDAC-g-SAH

Fig. 8 Variation of swelling Index with concentration of biopolymer.

Fig. 9 Variation of swelling index with respect to time.

Fig. 10 Swollen PDAC-g-SAH and Oven-dried PDAC-g-SAH.

Fig. 11 FT-IR spectra

Fig. 12 ^{13}C NMR spectra

Fig. 13 XRD spectra

Fig. 14 SEM images of hydrogels

Fig. 15 Thermogravimetric analysis spectra

Fig. 16 Rheological analysis graph

Fig. 17 WRC graph

Fig. 18 Release kinetics of dinotefuran by the K.P. model

Fig. 19 Release kinetics of dinotefuran by first-order kinetics

LIST OF TABLES

Table 1 Specifications of tannin

Table 2 Swelling index for various formulations of synthesized hydrogels.

Table 3 Release kinetics study for the encapsulation of pesticide dinotefuran in the hydrogel matrix

ABBREVIATION

PD *Prunus Domestica*

AC *Acacia Catechu*

SI Swelling Index

WRC Water Retention Capacity

KP Korsmeyer Peppas

PD-g-SAH *Prunus domestica* grafted sodium acrylate hydrogel.

AC-g-SAH *Acacia catechu* grafted sodium acrylate hydrogel

PDAC-g-SAH *Prunus domestica – Acacia Catechu* grafted sodium acrylate hydrogel.

CHAPTER 1

INTRODUCTION AND LITERATURE REVIEW

Agriculture is one of the global primary activities accounting for 70% of water usage [1].Studies claim that , during traditional methods of irrigation , almost 50% of this water is wasted due to evaporation, uneven distribution and surface runoff [2]. The remaining water, along with the soil nutrients, moves deeper in the soil and causes water stress in plants. Additionally, plants experience oxidative stress and increased lipid peroxidation due to limited water availability [3]. Lipid peroxidation leads to damage of cell membranes and loss of other important biomolecules such as proteins [4]. These stresses collectively lead to reduced plant growth, poor reproductive health and ultimately poor yield [5]. Therefore, there is a need for such materials which can improve the water efficiency by minimizing the water loss and helpful in maintaining the soil moisture in area of roots at the same time. Polymer-based hydrogels emerge as an effective solution for cutting water wastage in such scenario, as they can absorb and retain large amount of water. Hydrogels function as small water reservoirs, absorbing during rainfall and irrigation and releasing it during drought and shortage of water. This helps in limiting the leaching of nutrients due to water wastage and thus improve the crop productivity [6].

Along with water wastage, agriculture significantly contributes to the wastage of 90% of the pesticide applied on the crops due to a number of factors termed as mineralisation, biotransformation, leaching, and others [7]. These factors are highly responsible for decrement in crop yield and quality of the overall product. Pesticide application is helpful in protection of plants up to a great extent, but their wastages damage the environment and human life at a great extent, leading to issues such as cancers, respiratory tract issues, reproductive disorders, neurological disorders and

many issues related to immune system [8]. Thus, this creates a high demand for carriers, which are smart enough to extend the duration of pesticide release and prevent leaching into the soil [9]. This will also help in minimizing the usage of pesticides in the soil. Hereby, natural gum-based polymers emerge as a smart carrier to slow down the release of pesticide in the soil and thus extend its duration of use [7]. Since these are derived from natural materials, they contribute significantly to the sustainable environment. Encapsulating these chemicals into such carries would enhance their non target toxicity and reduce their degradation into the soil [10].

Hydrogels are three-dimensional crosslinked polymeric network, created by long polymer chains. These are highly hydrophilic in nature due to the presence of water loving functional groups such as - OH, -COOH, $-NH_2$, $-SO_3H$, $-CONH_2$, etc [11], [12] .This hydrophilic behaviour enriches them with the intrinsic property of absorbing a large amount of water, ranging up to 1000 times their actual dry weight. Many crosslinking techniques are employed in the formation of the hydrogel network such as hydrophobic interactions, hydrogen bonding, polymer entanglement, π–π stacking, free radical polymerisation, enzyme-induced crosslinking, etc [13]. There are various crosslinkers used in the production of hydrogels which are categorised as natural and synthetic crosslinkers. Natural crosslinkers include gallic acid (MW: 170.12 g/mol) , citric acid (MW: 192.12 g/mol), gnepine (MW: 255.23 g/mol) , etc. whereas synthetic crosslinkers involve the use of glutaraldehyde MW: 100.12 g/mol), Methylene bis-acrylamide (MW: 154.17 g/mol) , N-(3-dimethylaminopropyl)-N’ ethyl carbodiimide hydrochloride (MW: 191.70 g/mol) etc [14].

The absorbing capacity of hydrogels highly depend on the level of crosslinking. Highly crosslinked hydrogels form highly dense network which results in the formation of low absorbing polymer while low level of crosslinking produces highly absorbing hydrogels. Agriculture demands hydrogels which exhibit high swelling index as they can be beneficial during drought prone or low rainfall situations and also contribute in encapsulating the pesticide amount efficiently [14], [15]. Tannins, particularly obtained from the tress of *Acacia catechu*, is one class of natural

crosslinker, which provide crosslinking due to the presence of the polyphenolic groups. Tannins are capable of exhibiting various kind of interactions such as hydrophobic coordination, electrostatic interactions, hydrogen bonding, and ionic bonding, during crosslinking with hydrophilic polymeric network [16]. AC is basically a class of condensed tannins, with the crosslinking agents mainly composed of catechin, epicatechin, epigallocatechin, taxifolin, procyanidin, and quercetin [17]. Studies revealed that the monomers of AC are mainly catechin and epicatechin in the ratio of 4.2:1[18], [19]. **Figure 1(a**) and **1(b)** represent the monomer of AC and **Figure 2** represent the general structure of condensed tannins [20].

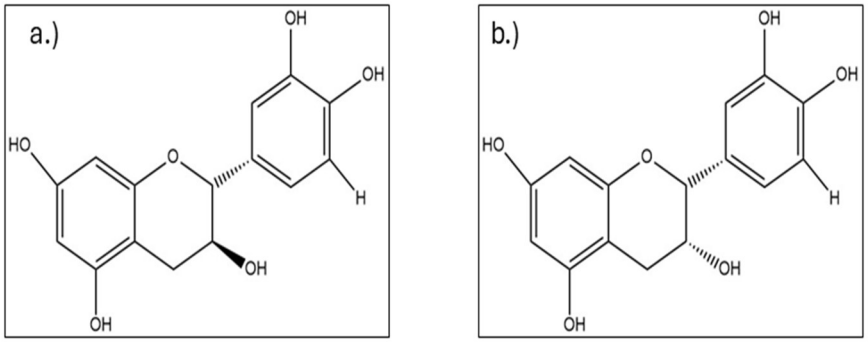


Figure 1: Structure for a) Catechin (b)Epicatechin

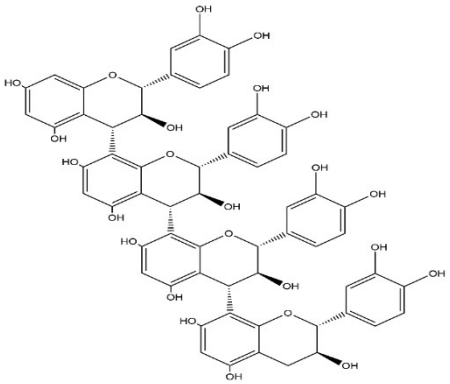


Figure 2: Structure for condensed tannins

Gum based hydrogels are an emerging category, highly explored for making hydrogels in the agricultural field due to their non toxicity and sustainability. These are explored in many other applications such as biomedical, wound healing, food packaging, cosmetics,

tissue engineering, etc [21], [22]. *Prunus domestica* is one such gum which is obtained from the plum tree of the *Rosaceae* family. This gum has 73% of water-soluble fractions and 27% of water insoluble fractions [23]. Past studies indicated that the backbone of PD is made up of galactose and arabinose, with small amounts of xylose and mannose [24]. As per the literature survey, this gum is not explored in many applications. **Figure 3** represents the raw image for PD gum.



Figure 3: Raw image of PD gum

Pesticide used in this study is chosen as dinotefuran. Dinotefuran is highly used, advanced-generation neonicotinoid with a large spectrum of activity. It is highly effective in controlling pests [25]. The chemical name of this compound is (RS)-1-methyl-2-nitro-3-(tetrahydro-3-furylmethyl) guanidine and the chemical structure is shown in **Figure 4** [26]. Being highly effective in controlling pests, there are some toxicity concerns associated with the chemical. It affects the life oof many animals such as honeybees, zebrafish, and *Bombyx Mori*. It also affects the human health by

incorporating into the food chain [27], [28]. Hence there is a release of slow release of dinotefuran to avoid over usage and longer benefits to the crops.

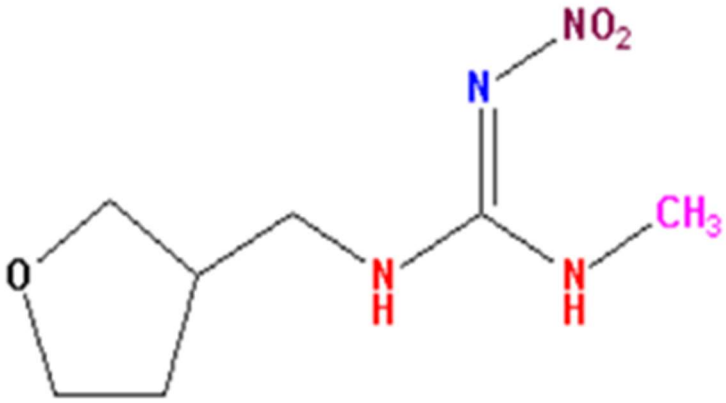


Figure 4: Chemical structure of dinotefuran

The present study focuses on synthesis and characterization of the *Prunus domestica* and Tannin grafted hydrogel by various spectroscopy techniques for the extended release of dinotefuran.

CHAPTER 2

MATERIALS AND METHODOLOGY

2.1 Materials

Prunus domestica Gum (PD) was imported from Iraq. Tannin (AC) was bought from Vaibhav Traders, Bawana Industrial Area, Delhi. Sodium hydroxide, acrylic acid, and N, N-Methylenebisacrylamide (MBA) were obtained from CDH Pvt. Ltd. Potassium persulfate (KPS) was sourced from SD Fine Chem Ltd. Dinotefuran was sourced from Institute of Pesticide Formulation and Technology, Gurugram.

2.2 Synthesis

In this study, PDAC-g-SAH, PD-g-SAH and AC-g-SAH hydrogels are synthesised via free radical polymerization using acrylic acid (AA), NaOH and N, N' MBA as crosslinker. The synthesis began with making of homogenous solutions of PD and AC in 15ml of deionised water. Then, AA (7ml), after neutralizing with 4.2g of NaOH, was added in the solution. The stirring continued and 0.1 g of KPS was added as initiator. MBA was added after 20-30 minutes and stirring continued for 2 hours. Afterwards, the hydrogels were solidified via hot water bath at 60°C for 60 minutes.

The hydrogels were sliced into discs and further submerged into deionized water to remove the excess chemicals. These hydrogels were further oven dried at 50°C and then stored in an air tight desiccator to prevent moisture and further use in application and characterization.

2.3 Swelling studies of the synthesised hydrogels

The swelling indices were calculated by immersing the oven dried hydrogels in distilled water. The swelling was observed for a duration of 42 hours. The weight of the hydrogels was noted down in dry state and then subsequently noted again after a specific duration of time after immersion in deionized water. This activity was

continued until a constant weight was recorded. **Table 2** shows the various formulations prepared in the study along with their swelling indices in the respective column.

The SI was calculated by the following **Equation 1** [29].

$$Swelling\ Index\ (g.g^{-1}) = \frac{Ws-Wd}{Wd} \quad (1)$$

where W_S is the weight of swollen hydrogel, and W_D is the weight of oven-dried hydrogel.

Swelling study was evaluated by varying concentration of biopolymer and time.

2.4 Characterization

All the synthesised hydrogels were characterised using FT-IR spectroscopy to determine the functional groups and bonding modes present among the molecules in the samples, using a Perkin-Elmer model 2000 FTIR spectrometer over the range 4000-650 cm^{-1}. Solid-state ^{13}C NMR was performed on a 400 MHz ECX-II JEOL spectrometer for molecular structural elucidation. Powdered XRD of hydrogels was examined for the crystal nature of the samples using from 10° to 2°/min using a Panalytical's X'Pert Pro diffractometer with Cu Kα radiation. SEM was performed to determine the surface morphology of the samples using an EVO 18 Research instrument (Zeiss). TGA was carried out using SDT650 (192.168.1.11). Further rheology was performed using Anton Paar Modular Compact Rheometer 302 (MCR). All the synthesised hydrogels were oven dried and grind to make a fine powder which was further used to carry out the characterization except for the rheological analysis.

2.5 Water Retention Capacity (WRC)

Water retention capacity of hydrogels can be defined as the maximum amount of water which can be hold and retained by the respective hydrogel. WRC studies were conducted to study more deeply about this interesting characteristic of the hydrogel network in presence of oven dried soil. A set up was arranged which consisted of

conical tubes, oven dried soil and 0.1g of powdered hydrogel of both the hybrid and the controls. Conical tubes were filled with soil up to a 45ml mark and then a layer of hydrogel was deposited over it. Then small portions of water were subsequently added at a specific interval of time and weights were recorded in all set ups. This process was continued for a duration of 7 days and the explicit behaviour of hydrogel network was recorded. Further the formula given in **Equation 2** was used to calculate the WRC% [30] and compare the performances of the hydrogels.

$$WRC\% = \frac{W_t - W}{W_O - W} \times 100 \quad (2)$$

Where W_t refers to the weight of the tube after the addition of water at time t.

W_O is the weight of the tube filled with dry soil and hydrogel layer in the absence of water.

W corresponds to the weight of the tube filled with soil only.

2.6 Encapsulation and release study of dinotefuran using PDAC-g-SAH, PD-g-SAH, and AC-g-SAH

Oven-dried hydrogels were measured in discs of 0.2g each and then these were put in a 720 ppm dinotefuran solution prepared in distilled water for a duration of 24 hours. Afterward, the hydrogels were taken out and termed as ‘loaded hydrogels. These hydrogels were put in deionized water (250ml) and measurements were recorded for complete 45 hours as the release was observed for 45 hours for the hydrogels. During the study, 3 ml of solution was removed from each beaker and stored safely for the UV-visible spectroscopy. Alongside, 3 ml distilled water was subsequently added to maintain the constant volume. The UV-visible spectrophotometer was used to calculate the concentration present in the solution at different time stamps, with the maximum absorption obtained at the wavelength of 271nm for dinotefuran [31].

2.6.1 Percentage loading

The percentage loading for the 'loaded hydrogels' was calculated using the formula given in **Equation 3**. This value indicates the amount of pesticide actually trapped within the polymeric network relative to the total pesticide concentration.

$$\% L = \left(\frac{A_L - A_R}{A_L}\right) * 100 \quad (3)$$

where A_L is the amount of dinotefuran added to the hydrogels.

A_R is the amount of dinotefuran remaining in the hydrogels.

CHAPTER 3

SPECIFICATIONS OF *PRUNUS DOMESTICA* AND TANNIN

3.1 *Prunus domestica*

PD was collected from the plum tree which belongs to the Rosaceae family in Iraq. Then it was cleaned by washing with deionized water to remove the dust, microbial and air impurities if present on its upper layer to avoid any contamination. Then it was sliced into small pieces and oven dried at 60°C temperature. Crushing of gum was carried out using a mortar and pestle to obtain an off-white-colored odorless powder with a few amounts of yellowish lumps in it as shown in **Figure 5**.



Figure 5: Powdered PD gum

Further ash%, purity% and yield% was calculated using various formulas.

3.1.1 Ash%

2g of PD was weighed and put in a muffle furnace at 550°C for 4-5 hours. The formula present in **Equation 4** was used to calculate the ash%

$$Ash\ \% = \frac{Weight\ of\ ash}{Weigh\ \ of\ sample} \times 100 \quad (4)$$

On substituting the data obtained, we got

$$Ash\ \% = \frac{0.07}{2} \times 100 = 3.5\%$$

3.1.2 Purity%

The purity percent of the gum was calculated by taking in account of ash% and formula present in **Equation 5** was used for this purpose.

$$Purity\ \% = 100 - Ash\% \quad (5)$$

Then we have,

$$Purity\ \% = 100 - 3.5\% = 96.5\%$$

3.1.3 Yield%

Yield% was calculated by taking in account of the formula provided in **Equation 6** [32].

$$Yield\ \% = \frac{Weight\ of\ extracted\ gum}{Weight\ of\ raw\ gum} \times 100 \quad (6)$$

The weights of extracted gum and raw gum were found to be 11 grams and 21 grams respectively. Thus, the yield% would be calculated as shown below.

$$Yield\ \% = \frac{11}{21} \times 100 = 52.3\%$$

3.2 Tannin

The tannin was bought from Vaibhav Traders, Bawana Industrial Area, Delhi. It was obtained as a fine brown colored powder without any lumps in it. **Figure 6** shows the texture and color of tannin.



Figure 6: Powdered form of tannin

The matter specifications were carried out by **CSIR** and results were obtained as shown in **Table 1**.

Table 1: Specifications of tannin

S.No.	Specified material	% composition
1.	Volatile matter	8%
2.	Total solid	92%
3.	Total soluble	84.1%
4.	Non-tannin content	26.7%
5.	Tannin content	57.4%
7.	Water insoluble	7.9%
7.	Water solubility pH	5.5%

Literature survey confirms that the number and mass average molecular weight of *Acacia catechu* are 914g mol^{-1} and 1407g mol^{-1} respectively. The polydispersity index is 1.54 which confirms the presence of non-uniform polymeric chains in the network [18].

CHAPTER 4

RESULTS AND DISCUSSION

4.1 Reaction Mechanism

KPS acts as an initiator which generates free radicals, which further react with the vinyl groups of sodium acrylate resulting in formation of poly(sodiumacryalte) chains. These chains propagate and reacts with the monomer (PD and AC) and crosslink together with the help of N, N'- MBA resulting in the formation of PDAC-g-SAH, PD-g-SAH and PDAC-g-SAH [33], [34]. **Figure 7** reflects the mechanistic pathway of the formation of the PDAC-g-SAH. The polymeric chains expand prominently due to electrostatic repulsion among the negatively charged carboxylate ions spaced in the polymer chains [35].

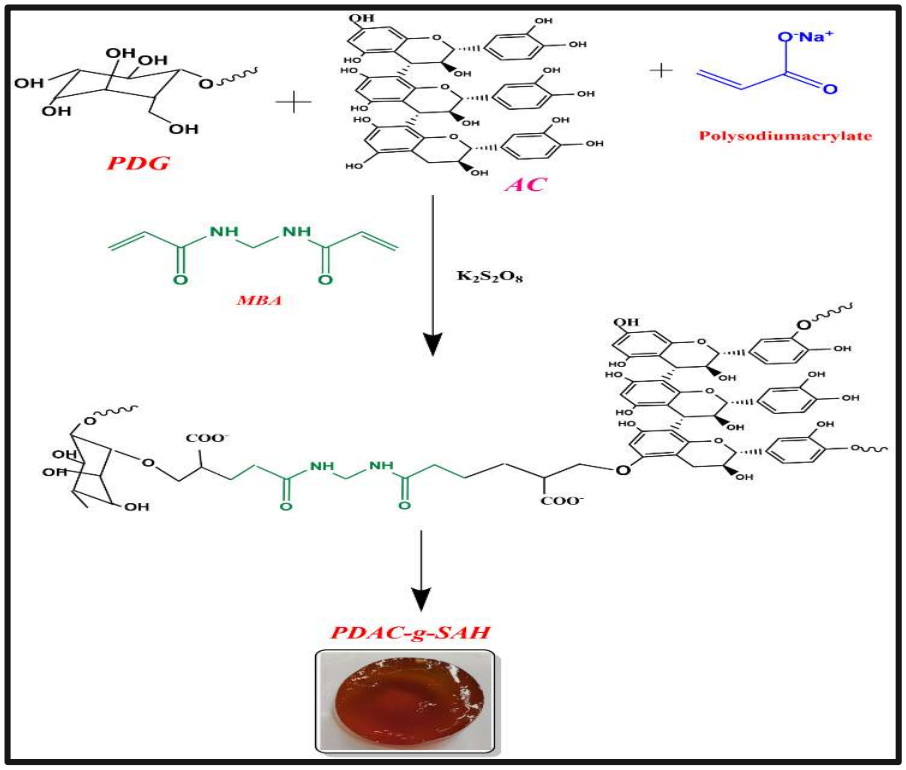


Figure 7: Mechanistic pathway of formation of PDAC-g-SAH

KPS molecule cleave to generate radicals.

$$K_2S_2O_8 \rightarrow 2K^{\cdot} + S_2O_8^{\cdot} \rightarrow 2SO_4^{\cdot}$$

These radicals attack the PD and tannin units [36].

Here, PD is denoted as R-PD-OH, and tannin is denoted as AC-OH.

The formation of PD-g-SAH and AC-g-SAH follows the below provided pathway.

$$R - PD - OH + 2SO_4^{\cdot} \rightarrow R - PD - O^{\cdot} + HSO_4^{\cdot}$$

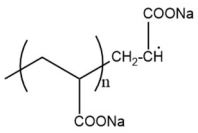
$$AC - OH + 2SO_4^{\cdot} \rightarrow AC - O^{\cdot} + HSO_4^{\cdot}$$

Simultaneously the active sites of sulphate group attacks the vinyl group of sodium acrylate and forms the Poly-(sodium acrylate).

$$CH_2 = CH - COONa + SO_4^{\cdot} \rightarrow NaOOC - CH^{\cdot} - CH_2^{\cdot} + SO_4^{\cdot}$$

The second step is the propagation step, which begins with the formation of extended Poly(sodium acrylate) chains.

$$n(CH_2 = CH - COONa) + NaOOC - CH^{\cdot} - CH_2^{\cdot} \rightarrow$$



Simultaneously the radicals of PD and AC react with acrylic acid and MBA to generate a grafted network [37].

$$CH_2 = CH - COONa + R - PD - O^{\cdot} \rightarrow NaOOC - CH^{\cdot} - CH_2^{\cdot} - O - PD - R$$

$$CH_2 = CH - COONa + AC - O^{\cdot} \rightarrow NaOOC - CH^{\cdot} - CH_2^{\cdot} - O - AC$$

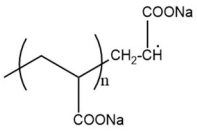
$$MBA + R - PD - O^{\cdot} \rightarrow MBA^{\cdot} - O - PD - R$$

$$MBA + AC - O^{\cdot} \rightarrow MBA^{\cdot} - O - AC$$

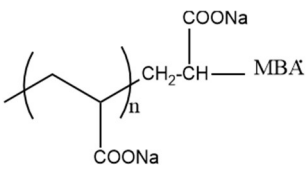
$$AC - OH + R - PD - O^{\cdot} \rightarrow R^{\cdot} - PD - O - O - AC$$

Poly(sodium acrylate) radicals react with the MBA molecules to produced 2d branched polymer

MBA +

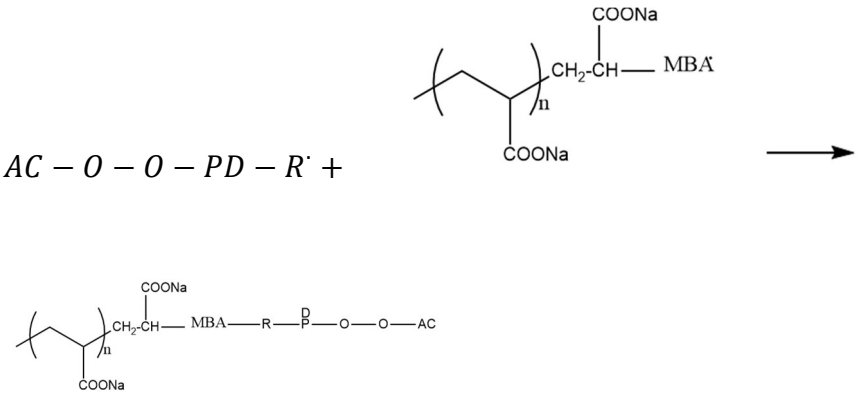


→

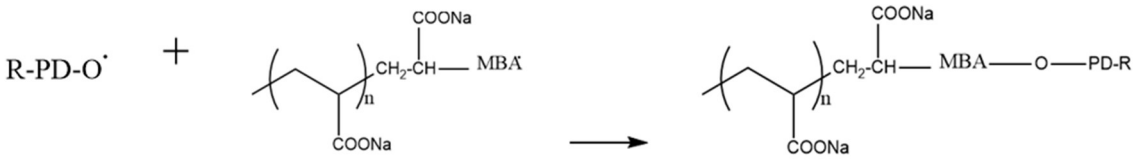


Now the termination step proceeds as two polymer chains integrate. Subsequently, PD-g-SAH , AC-g-SAH, and PDAC-g-SAH are formed via crosslinking with MBA, giving rise to a 3D polymeric network [32], [38].

a) PDAC-g-SAH



b) PD-g-SAH



c) AC-g-SAH



4.2 Swelling study

The swelling data as present in **Table 2** shows that PDAC-g-SAH had SI ($g \cdot g^{-1}$) of 219.83 ($g \cdot g^{-1}$) in 42 hours. For other hydrogels, PD-g-SAH (142.8 $g \cdot g^{-1}$) was observed after 37 hours, and AC-g-SAH (100.36 $g \cdot g^{-1}$) after 35 hours. From the study, it was concluded that PDAC-g-SAH exhibited the highest SI and longest sustained period for swelling.

Table 2: Swelling index for various formulations of synthesized hydrogels.

S.No.	Formulation	PD(g)	AC (g)	AA (ml)	NaOH (mol L^{-1})	KPS (g)	MBA (g)	SI ($g \cdot g^{-1}$)
1	PDAC-g-SAH 1	0.1	0.1	7.2	10.5	0.1	0.08	159.45
2	PDAC-g-SAH 2	0.2	0.1	7.2	10.5	0.1	0.1	132.5
3	PDAC-g-SAH 3	0.3	0.1	7.2	10.5	0.1	0.12	219.83
4	PDAC-g-SAH 4	0.4	0.1	7.2	10.5	0.1	0.15	110.45
5	PDAC-g-SAH 5	0.1	0.2	7.2	10.5	0.1	0.2	81
6	PDAC-g-SAH 6	0.2	0.2	7.2	10.5	0.1	0.08	154.4
7	PDAC-g-SAH 7	0.3	0.2	7.2	10.5	0.1	0.14	148.4
8	PDAC-g-SAH 8	0.4	0.2	7.2	10.5	0.1	0.12	122.52
9	PDAC-g-SAH 9	0.1	0.3	7.2	10.5	0.1	0.12	215.35
10	PDAC-g-SAH 10	0.2	0.3	7.2	10.5	0.1	0.14	181.4
11	PDAC-g-SAH 11	0.3	0.3	7.2	10.5	0.1	0.08	194.45
12	PDAC-g-SAH 12	0.4	0.3	7.2	10.5	0.1	0.1	103.65
13	PDAC-g-SAH 13	0.1	0.4	7.2	10.5	0.1	0.14	116.31
14	PDAC-g-SAH 14	0.2	0.4	7.2	10.5	0.1	0.12	171.15
15	PDAC-g-SAH 15	0.3	0.4	7.2	10.5	0.1	0.1	98.36
16	PDAC-g-SAH 16	0.4	0.4	7.2	10.5	0.1	0.08	126.7
17.	PD-g-SAH	0.4	0	7.2	10.5	0.1	0.12	142.8
18.	AC-g-SAH	0	0.4	7.2	10.5	0.1	0.1	100.36

4.2.1 Effect of concentration of biopolymer on SI

The biopolymer concentration was varied between 0.1 and 0.4g. A Gradual increase in swelling index was observed as concentration of biopolymer was increased, taking crosslinker as constant as shown in **Figure 8**. But SI did not increase when biopolymer was increased above 0.3g [39].This trend can be attributed to the formation of dense polymer network at high biopolymer content which lowers the available free volume in the network and limits the water absorption capacity [28], [40].

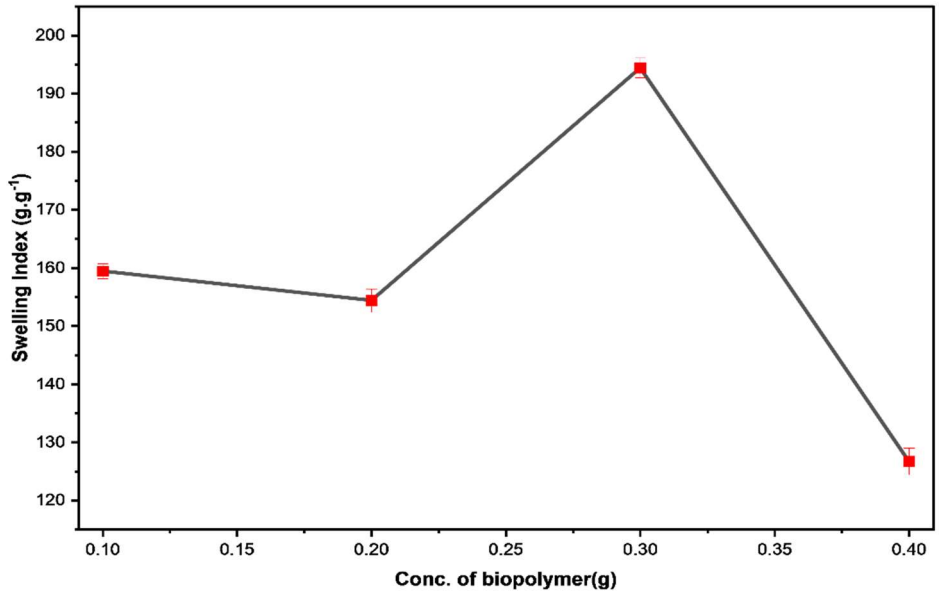


Figure 8: Variation of swelling Index with concentration of biopolymer.

4.2.2 Variation of SI with respect to time

The swelling index was gradually observed during immersion and increased, as shown in **Figure 9**. However, the increase rate was higher in the initial hours but it become almost constant as time increases. The rapid swelling is accounted as the difference in osmotic pressure between the polymeric network and outside environment. The swelling is mainly a result of presence of multiple hydrophilic chains, countercharged species and static charge in the polymeric network [41].

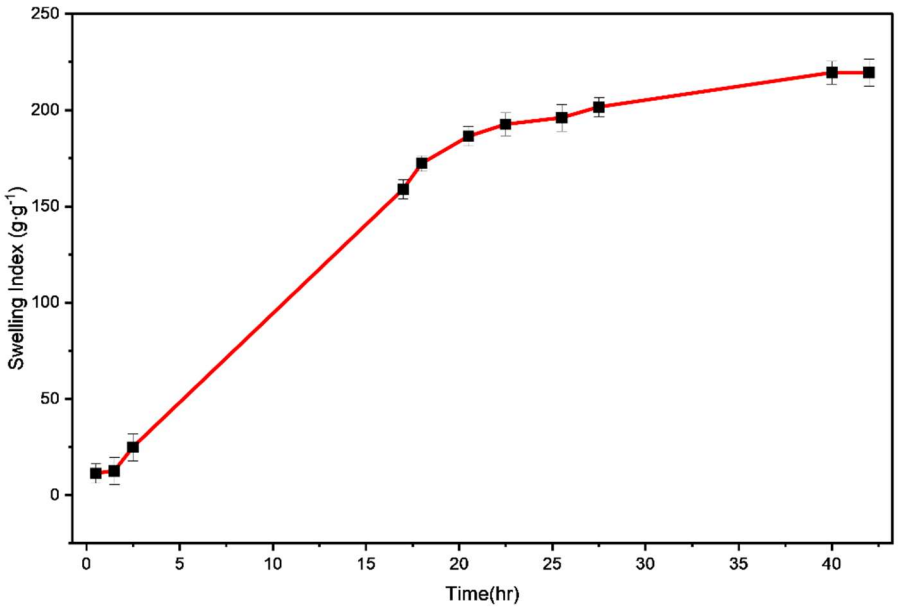


Figure 9: Variation of swelling index with respect to time.

4.3Physical features of the synthesized hydrogel

Synthesized hydrogels depicted different physical properties in their swollen and dry states. The appearance of the hydrogels can be evaluated from **Figure 10**. The significant color of hydrogels is due to the presence of tannin in it. However, the weight, height, diameter, and volume for swollen state were found to be 60.09 g, 3.5 cm, 5.1 cm, and 69.42 cm^3, respectively, while in the dry state, these were 3.59 g, 0.8 cm, 1.2 cm, and 0.91 cm^3, respectively. The increase in hydrogel volume is due to the increase in diameter of pores and encapsulation of water molecules.

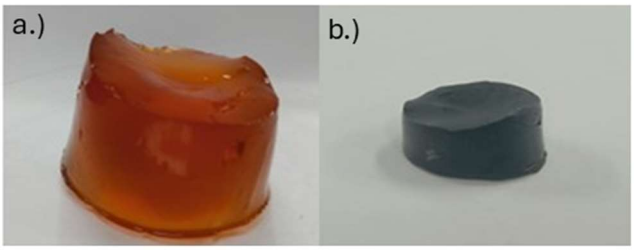


Figure 10: a) Swollen PDAC-g-SAH and b) Oven-dried PDAC-g-SAH.

4.4 Characterization

4.4.1 FT-IR

Figure 11 shows the FT-IR spectra of PD-g-SAH, AC-g-SAH, and PDAC-g-SAH. There were peaks in the 4000 cm^{-1} to 600 cm^{-1} regions in the FT-IR spectra. OH stretching was identified as broad peaks in all formulations at 3325, 3301, and 3317 cm^{-1} in all manufactured hydrogels, while sp^3 hybridized C-H stretching, which indicating chains of hydrocarbons, was observed for the notable peak at 2917, 2936, and 2927 cm^{-1}. The COOH group and, thus, acrylate is shown by the peaks at 1717, 1718, and 1719 cm^{-1}. The carbonyl stretching mode of MBA is represented by the peaks at 1559, 1563, and 1558 cm^{-1} [42]. C-O-C stretching was identified by the peaks at 1174, 1160, and 1164 cm^{-1}, whereas the glycosidic band vibration is confirmed by the peak that emerged at 1036, 1030, and 1039 cm^{-1} [43], [44]. The peak at 1403, 1404, and 1403 cm^{-1} is caused by the symmetric COO-stretching vibration of the -C=O group of acrylate [45]. The existence of PD in the PDAC-g-SAH network is confirmed by the peak at 839 cm^{-1} which is in the fingerprint region and points towards α-α-glycosidic linkages [46], [47].

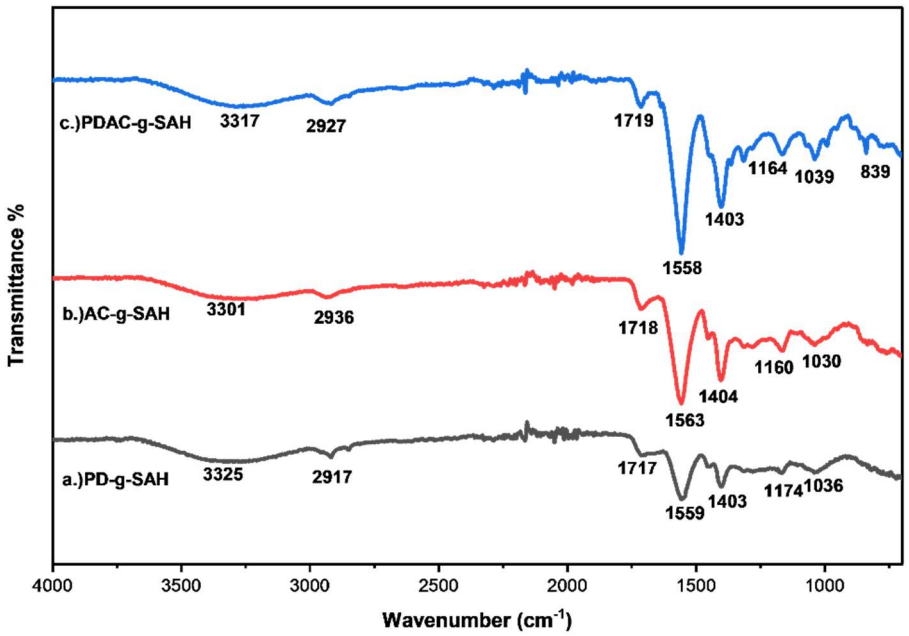


Figure 11: FT-IR spectra of a) PD-g-SAH, b) AC-g-SAH, and c) PDAC-g-SAH.

4.4.2 Solid-state ^{13}C NMR

Figure 12(a), **12(b)** and **12(c)** corresponds to the solid-state ^{13}C NMR spectra of PD-g-SAH, AC-g-SAH, and PDAC-g-SAH respectively. Figure 12(a) shows peaks at 42.232 ppm from the N, N-MBA group and at 184.943 ppm due to grafting with poly(sodium acrylate) [48]. Figure 12(b) also shows similar deviating peaks at 38.063 ppm and 181.671 ppm, respectively, showing the presence of N, N–MBA, and poly (sodium acrylate). The presence of C-6 of β-galactopyranosyl and anomeric C-1 carbon of 1,6-linked β-galactopyranosyl, 1,3-linked β-galactopyranosyl, β-arabinofuranose, β-β arabinofuranose, and 1,3-linked α-arabinofuranose residues is also visible in same region at 60.434 ppm and 108.206 ppm. The region of PDAC-g-SAH visible in Figure 12(c) shows three sharp peaks at 39.542 ppm due to N, N-MBA, 61.302 ppm due to biopolymer tannin, and 184.289 ppm, which is due to presence of poly(sodium acrylate). As similar peaks are retained in spectra of PDAC-g-SAH, this confirms the grafting of PD with AC in the formation of PDAC-g-SAH [49], [50].

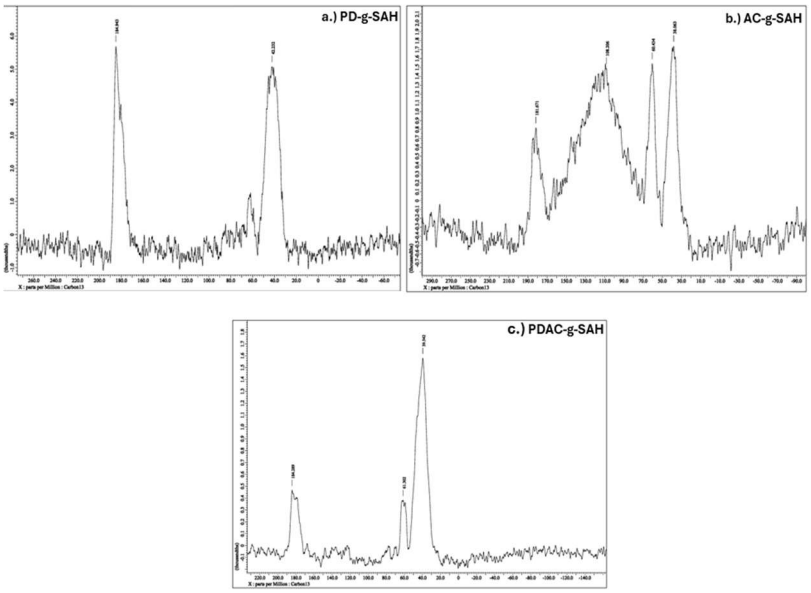


Figure 12: NMR spectra of a.) PD-g-SAH b.) AC-g-SAH, and c.) PDAC-g-SAH.

4.4.3 XRD

XRD was used to ascertain if the materials were crystalline or amorphous. **Figure 13** depicts the XRD patterns of PD-g-SAH, AC-g-SAH, and PDAC-g-SAH, with peaks at 21.86 ° and 32° in Figure 13(a) 20.05° and 31.84° in Figure 13(b), and 19.14° and 31.84° in Figure 13(c), were indicating towards the amorphous nature of all the synthesized hydrogels and grafting of poly (sodium acrylate) respectively [51] . The amorphous nature of all hydrogels is beneficial, as it enables high water absorption and chain mobility, which are essential for agricultural and other applications.

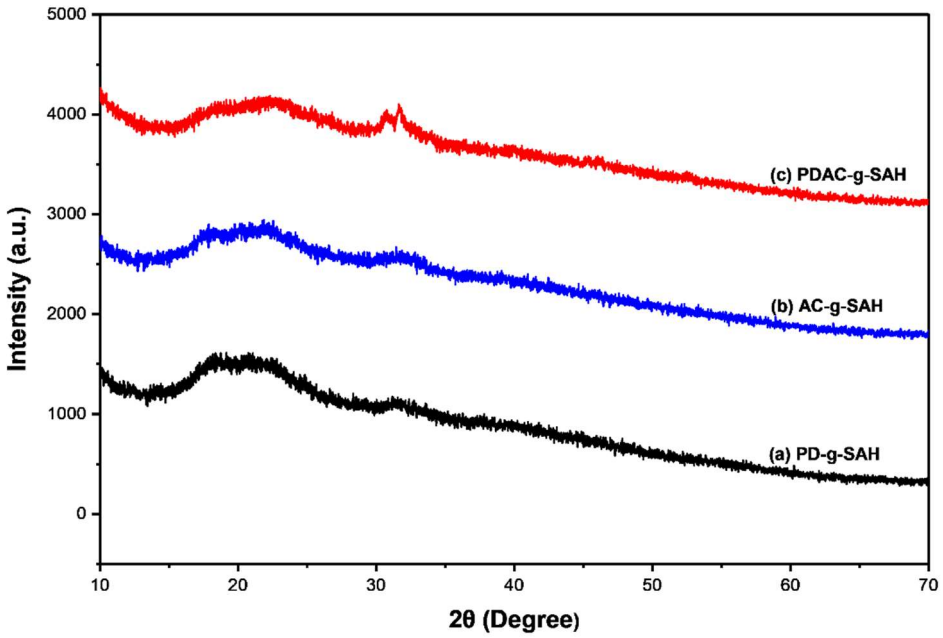


Figure 13: XRD pattern of a) PD-g-SAH, b) AC-g-SAH, and c) PDAC-g-SAH.

4.4.4 SEM

The surface morphology of PD-g-SAH, AC-g-SAH, and PDAC-g-SAH using SEM at 500x, 500x, and 1000x resolutions, as shown in **Figure 14(a)**, **14(b)**, and **14(c)**, respectively. SEM images show the porous structure of PDAC-g-SAH, which has larger pores than PD-g-SAH and AC-g-SAH. This discrepancy is probably due to the dense polymer network in PD-g-SAH and AC-g-SAH, which leads to strong intermolecular interactions and a packed, rather than porous, morphology. These pores provide synthetic hydrogels their gel-like characteristics and are the cause of the initial increased swelling rate because water enters the macro pores first, filling the micro pores later [52], [53].

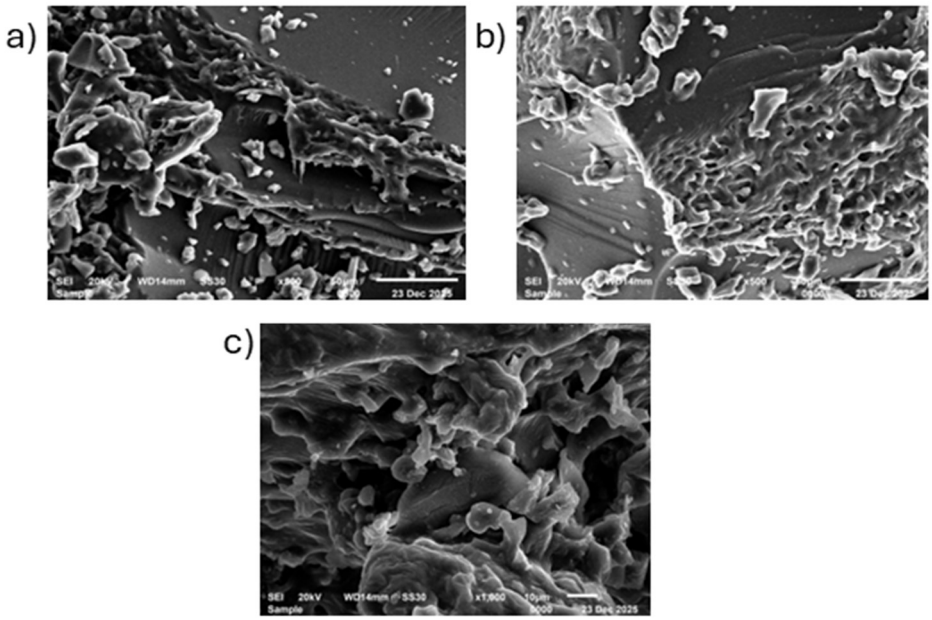


Figure 14: SEM images of a) PD-g-SAH, b) AC-g-SAH, and c) PDAC-g-SAH

4.4.5 TGA

The thermal stability of hydrogels was characterized using thermogravimetric analysis in the range of 25 ºC to 600 ºC. As shown in **Figures 15(a)**, **15(b)**, **and 15(c)**, four transition phases were observed in the thermal degradation. With mass losses of 8.9%, 7.7%, and 8.4% for PD-g-SAH, AC-g-SAH, and PDAC-g-SAH, respectively, the first phase starts at 28 ºC –209 ºC, 27 ºC –207.91 ºC, and 27.63 ºC –218 ºC. This stage is associated with the evaporation of water and the heating of low molecular weight molecules. Second stage degradation takes place between 209 ºC and 421 ºC, 207.91 ºC and 420 ºC, and 218 ºC and 411 ºC, with losses of 23.5%, 14%, and 16.7% for PD-g-SAH, AC-g-SAH, and PDAC-g-SAH, respectively. During this stage, certain ungrafted small molecules and the polymeric network's backbone degrade. Additionally, this degradation can be linked to the hydrogel matrices' methylene, alcoholic, and carboxylic groups [38], [54].

With weight loss percentages of 25.9%, 21.8%, and 24.1% for PD-g-SAH, AC-g-SAH, and PDAC-g-SAH, respectively, the third phase of degradation was seen between 421 ºC and 498 ºC, 420ºC and 500 ºC, and 411 ºC and 494.2 ºC, corresponding to the degradation of the polymeric network at its maximum. Strongly stable entities in the polymeric chain cause a relatively slight weight loss in the last stage of breakdown, up to 2.3% at 590 ºC [37]. The residue percentages of PD-g-SAH, AC-g-SAH, and PDAC-g-SAH were determined to be 40.5%, 50.94%, and 51.5%, respectively, indicating their heat resistance.

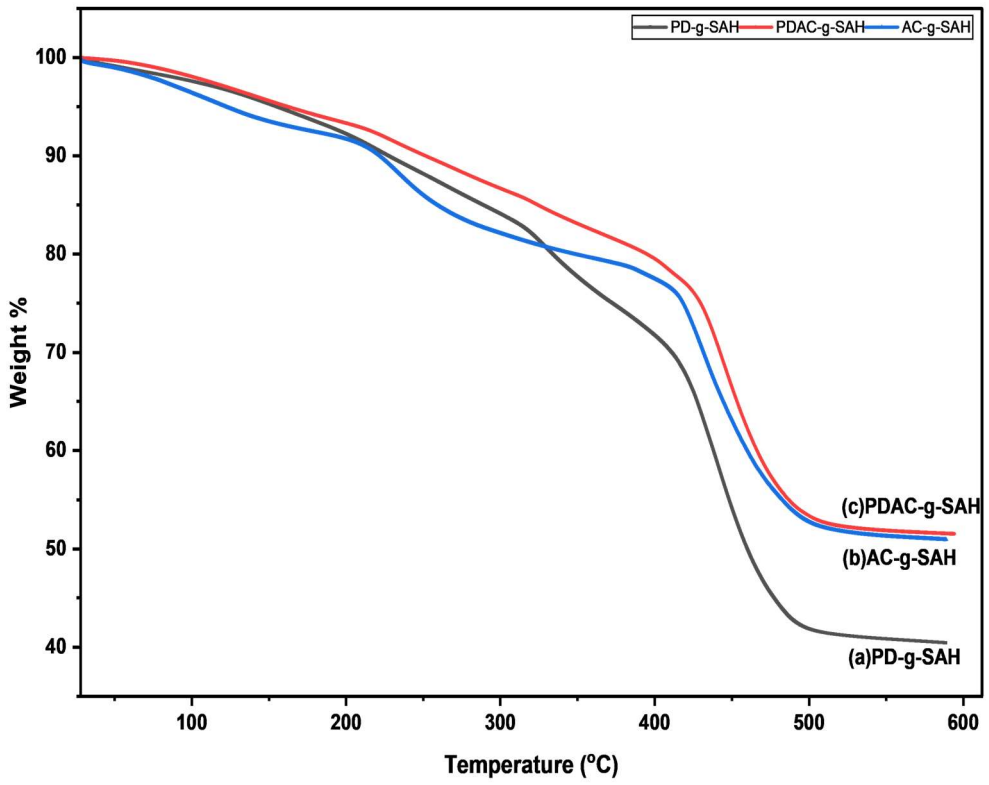


Figure 15: Thermogravimetric analysis for a) PD-g-SAH b) AC-g-SAH, and c) PDAC-g-SAH

4.4.6 Rheology

All the samples were subjected to shear stress amplitude at a rate of 10 rad/s during the amplitude sweep test. Results are shown in **Figure16[A] (a)**, **16[A](b)**, and **16[A](c)** for PD-g-SAH, AC-g-SAH, and PDAC-g-SAH respectively. The hydrogel

network is intact, as evidenced by the G″ and G′ being constant at mild deformation. We refer to this area as the linear-viscoelastic zone. Additionally, the termination of this region indicates that the structure is disrupted as the modulus decreases. When compared to PD-g-SAH and AC-g-SAH1, PDAC-g-SAH exhibits more viscoelastic solid behaviour [7] .

Additionally, the samples underwent frequency sweep test with constant shear strain percentage between 0.1 and 500 rad/s. **Figures 16[B] (a)**, **16[B] (b)**, and **16[B] (c)** show the results for PD-g-SAH, AC-g-SAH, and PDAC-g-SAH, respectively. According to this study, the synthesized hydrogel network's viscoelastic behaviour was demonstrated by the loss modulus, G″, being dominant at higher frequencies while the storage modulus, G′, was prominent at lower frequency areas [39].

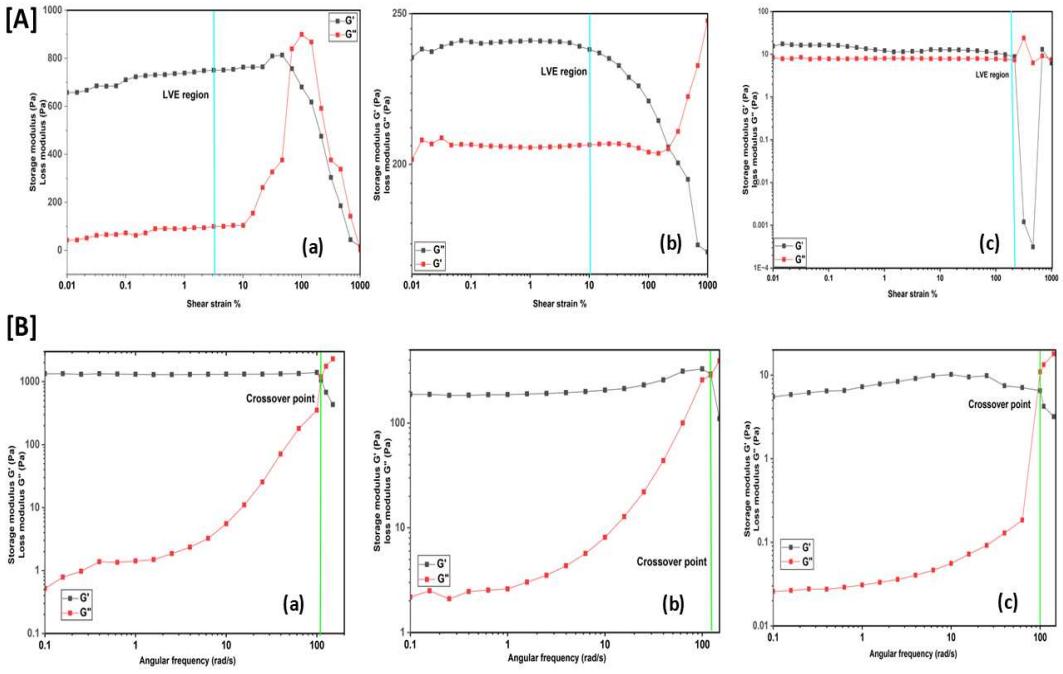


Figure 16: Rheological analysis of [A] amplitude sweep a) PD-g-SAH b) AC-g-SAH c) PDAC-g-SAH and [B] Frequency sweep of a) PD-g-SAH b) AC-g-SAH c) PDAC-g-SAH

4.5 Water Retention Capacity

Figure 17(a),**17(b)** ,**17(c)**, and **17(d)** represent the WRC% of PDAC-g-SAH, PD-g-SAH, AC-g-SAH, and control respectively. Results obtained showed that the WRC of soil was improved up to twice on implementation of hydrogel in the soil. The soil's WRC in untreated soil was found to be 23.1% on the 7th day. While in PDAC-g-SAH, PD-g-SAH, and AC-g-SAH it was found to be 42.2%, 34.4%, and 25.6%, respectively, on the seventh day. The result can be explained by the hydrophilic nature and crosslinking capacity of hydrogels, which are primarily responsible for encapsulating water molecules within the matrices. As a result, soil water availability is increased, which results in effective water usage and reduced moisture loss% in soil during evaporation [12].

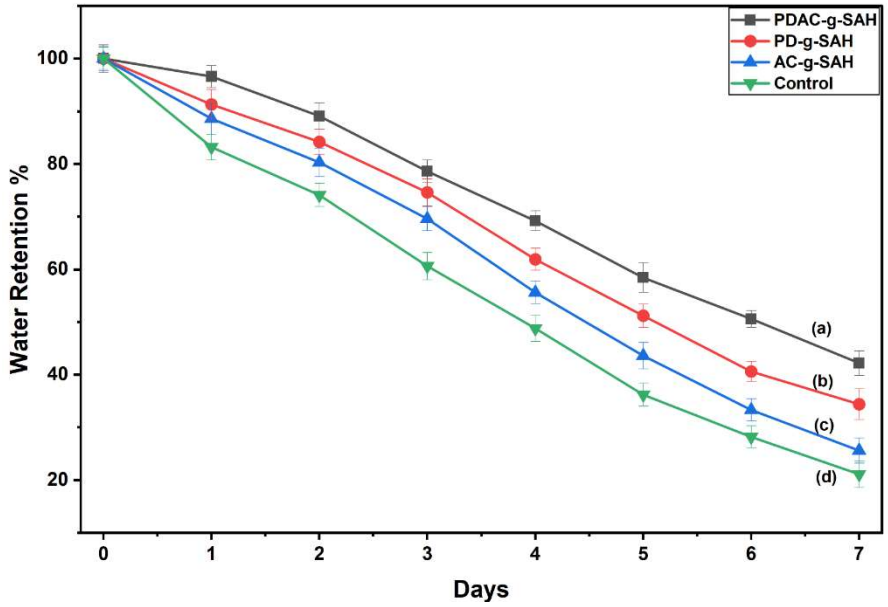


Figure 17: Water retention capacity of a) PDAC-g-SAH b) PD-g-SAH c) AC-g-SAH d) Control

4.6 Encapsulation of dinotefuran and release kinetics

4.6.1 Percentage loading

The % L of all synthesized hydrogels i.e. PDAC-g-SAH, PD-g-SAH, and AC-g-SAH were 54.97%, 47.27%, and 31.49% respectively. The higher %L can be attributed

due to the porous structure and high swelling index of the hydrogel matrices, enabling the dinotefuran molecules to penetrate deeply into the network of hydrogel.

4.6.2 Release Kinetics

The release study revealed that the dinotefuran was released for a duration of 48-50hours from the hydrogel matrix.

Release kinetics were studied using the Korsmeyer Peppas (KP) model, the Higuchi and first-order kinetics models. The KP model describes the release on the basis of the release exponent. In cylindrical systems, release exponent (n), $0<n<45$, would indicate Fickian diffusion while $45<n<0.89$ would point towards non Fickian diffusion. But if $n>0.89$, this is the case for super case II transport [55].. The only condition for KP model is that all the release must be less than or equal to 60%. Fickian diffusion indicates that the drug has been released through the matrix by diffusion, while non-Fickian diffusion reflects that the drug has been released as a result of diffusion and relaxation of the carrier matrix [56], [57]. **Figure 18** represent the graphs for KP model.

The Higuchi Model indicate that the dinotefuran has released by diffusion mechanism. It studies release in terms of square root of time[58].Further, first order kinetics states that the rate is directly proportional to the amount of pesticide remaining in the hydrogel matrix [59].The fitting of models is related by calculating the correlation coefficient ($R^2 > 0.97$). It is clear from **Table 3** that PD-g-SAH and AC-g-SAH satisfies the Fickian diffusion ($n < 0.45$) and first-order kinetics. Despite Fickian diffusion, the Higuchi model is unsatisfactory due to the shape of the hydrogel network, the pesticide release dimensions, and the hydrogel's swelling behavior. It takes in account that the polymer matrix does not swell or dissolve in the medium while releasing[60]. PDAC-g-SAH reflects the non-Fickian diffusion ($0.45<n<0.89$) and satisfies the first-order kinetics. **Figure 19** shows the graphs for first order kinetics. Also, the equations and rate constants obtained in release kinetics are shown in Table 3.

Table 3: Release kinetics study of prepared hydrogel matrix

S.n.	Model	Equation	Parameters	Values PD-g-SAH	Values AC-g-SAH	Values PDAC-g-SAH
1.	Korsmeyer Peppas	$M_t/M_\infty = K_{K.P.} t^n$ M_t/M_∞ is the amount of pesticide released, $K_{K.P.}$ is the Korsmeyer Peppas constant, n is the release exponent, and t is the time	R^2 $K_{K.P.}$ (hr^{-n}) n	0.99 0.0066 0.36	0.99 0.0069 0.35	0.99 0.00064 0.64
2.	Higuchi Model	$M_t/M_\infty = K_H\sqrt{t}$ M_t/M_∞ is the amount of pesticide released, K_H is the Higuchi constant, and t is the time	R^2 K_H ($hr^{-1/2}$)	0.89 0.11	0.90 0.091	0.905 0.21
3.	First-order kinetics	$M_t/M_\infty = 1- e^{-kt}$ M_t/M_∞ is the amount of pesticide released, K_1 is the first order constant, is and t is the time	R^2 K_1 (hr^{-1})	0.99 0.013	0.98 0.013	0.97 0.031

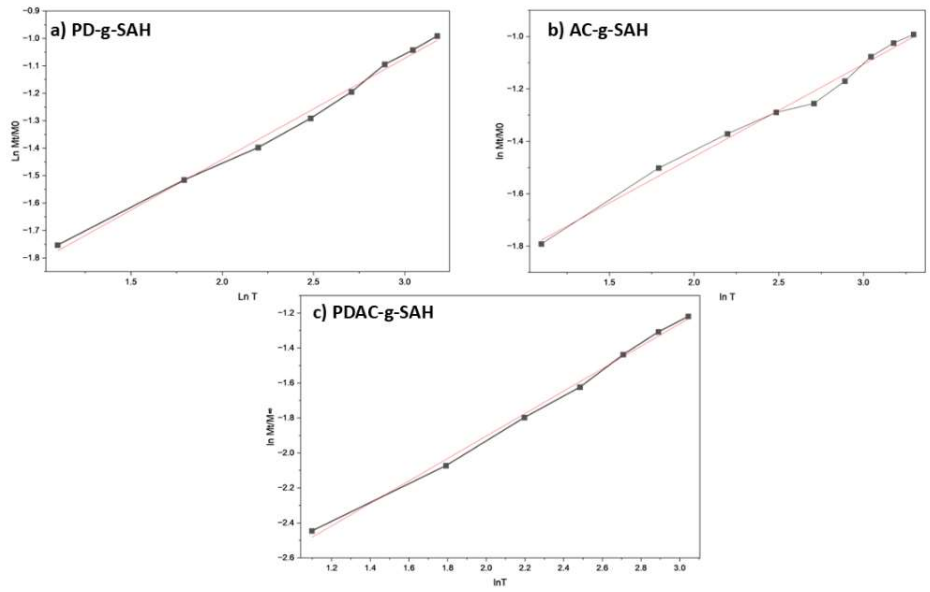


Figure 18: Release kinetics of dinotefuran by the Korsmeyer Peppas model for a.) PD-g-SAH b.) AC-g-SAH c.) PDAC-g-SAH.

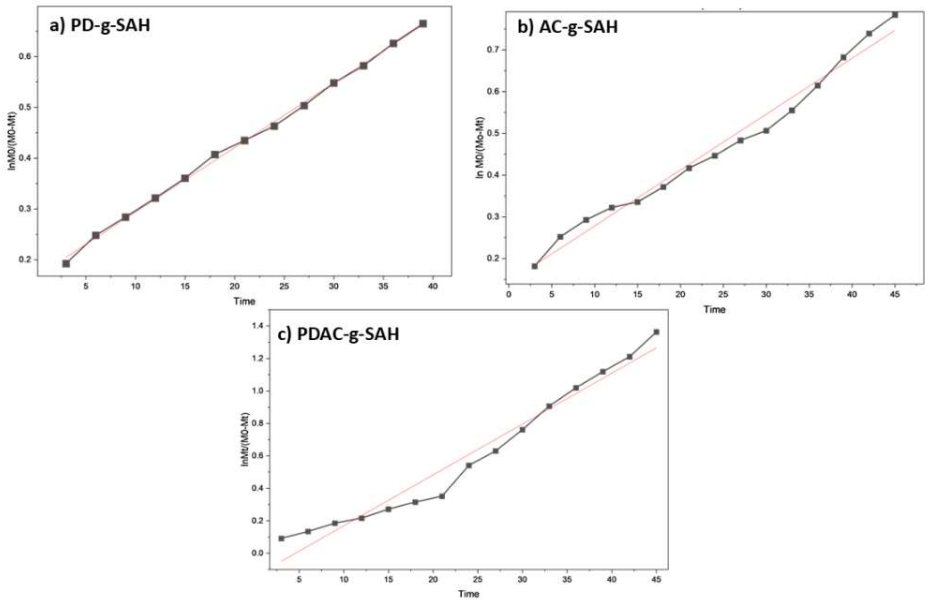


Figure 19: Release kinetics of dinotefuran by first-order kinetics for a.) PD-g-SAH b.) AC-g-SAH c.) PDAC-g-SAH.

CHAPTER 5

CONCLUSION AND FUTURE PROSPECTS

The present study focuses on development of novel biodegradable hydrogels synthsized from PD and AC for the controlled relaese of dinotefuran, aiming for improved pestcide efficieny while reducing environmental contamination due to soil leaching. Conventional pesticide formulations often lead to poor utilization due to rapid relaese. To address these issues, the study primarily focused on the synthesis and evaluation of PDAC-g-SAH hydrogel and compared its performance with PD-g-SAH and AC-g-SAH to establish the superior efficiency of PDAC-g-SAH as a controlled-release carrier system for agrochemical applications.

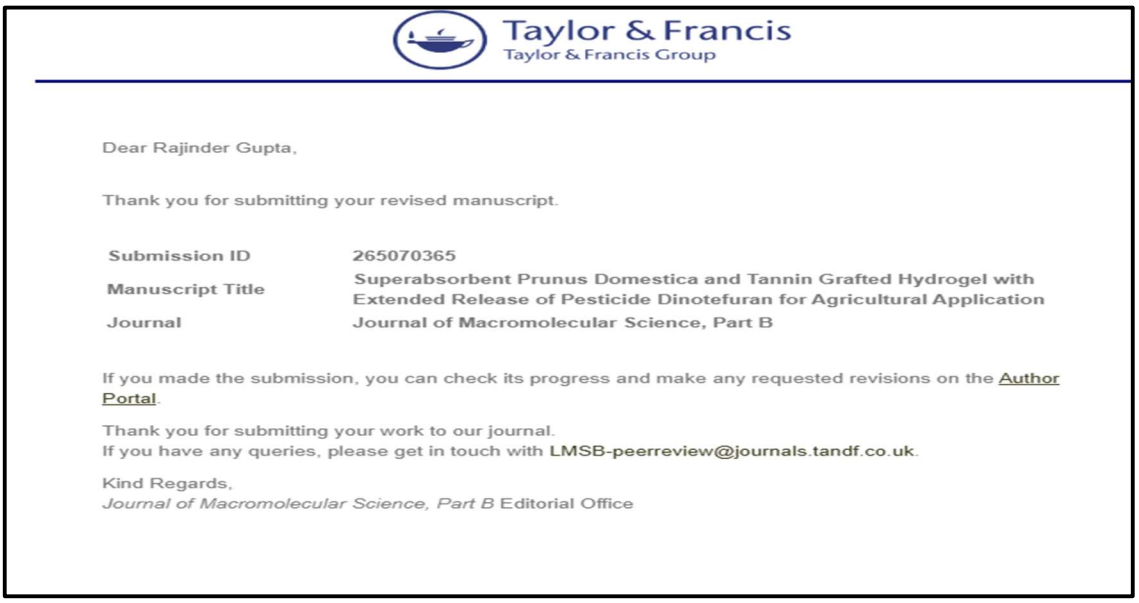
The synthesized hydrogels were characterized using several analytical techniques, including FT-IR, ^{13}C NMR, XRD, SEM, TGA, and rheological analysis. FT-IR and ^{13}C NMR confirmed the process of rafting of PD with AC while XRD revealed the crystal structucture of polymeric network.SEM images proved the porous network created by the hydrogel network, beneficial for higher water absorption capacity and encapsulation of pesticide.TGA demonstated the thermal stablity of polymer network and rheology established the viscoelastic behaviour of the network.

Among all synthesized formulations, PDAC-g-SAH exhibited the highest swelling index of 219.83 $g \cdot g^{-1}$, indicating its excellent water absorption capacity and enhanced hydrogel network structure. The hydrogel also showed superior water retention capacity, pesticide loading efficiency, and prolonged release behavior compared to PD-g-SAH and AC-g-SAH. The sustained-release profile of dinotefuran from PDAC-g-SAH ensured gradual, controlled delivery over an extended period, thereby minimizing pesticide loss through leaching and improving overall utilization efficiency. These properties highlight the effectiveness of PDAC-g-SAH as an advanced carrier system for agrochemical delivery.

Furthermore, the potential of these hydrogels can be leveraged beyond pesticide applications. Due to their high absorption values, they can be used as soil conditioners to improve soil moisture content, promote nutrient availability and seed germination , and support plant growth under drought situations.Hence, this research opens the door for new possibilities for the development of multifunctional hydrogels for sustainable agriculture , efficient pesticide management, and a barrier to environmental degradation.

JOURNAL PUBLICATION

Revised manuscript for the paper titled "**Superabsorbent *Prunus domestica* and Tannin Grafted Hydrogel with Extended Release of Pesticide Dinotefuran for Agricultural Application**" has been submitted to **Journal of Macromolecular Science, Part B.**



Taylor & Francis
Taylor & Francis Group

Dear Rajinder Gupta,

Thank you for submitting your revised manuscript.

Submission ID	265070365
Manuscript Title	Superabsorbent Prunus Domestica and Tannin Grafted Hydrogel with Extended Release of Pesticide Dinotefuran for Agricultural Application
Journal	Journal of Macromolecular Science, Part B

If you made the submission, you can check its progress and make any requested revisions on the Author Portal.

Thank you for submitting your work to our journal.
If you have any queries, please get in touch with LMSB-peerreview@journals.tandf.co.uk.

Kind Regards,
Journal of Macromolecular Science, Part B Editorial Office

DELHI TECHNOLOGICAL UNIVERSITY

(Formerly Delhi College of Engineering)

Shahbad Daulatpur, Main Bawana Road, Delhi- 42

PLAGIARISM VERIFICATION

Thesis titled with "**Superabsorbent *Prunus domestica* and Tannin Grafted Hydrogel with Extended Release of Pesticide Dinotefuran for Agricultural Application**".

This is to report that the above thesis was scanned for similarity detection. Process and outcome are given below:

Software: **Turnitin**

Similarity Index:

Total Word Count:

Date:

Prerna Gupta
(24/MSCCHE/18)

Prof. R. K. Gupta and Prof. D Kumar
(Supervisor)

RFERENCES

[1] C. Ingrao, R. Strippoli, G. Lagioia, and D. Huisingh, “Water scarcity in agriculture: An overview of causes, impacts and approaches for reducing the risks,” *Heliyon*, vol. 9, no. 8, p. e18507, 2023, doi: 10.1016/j.heliyon.2023.e18507.

[2] M. A. Ashour, Y. M. Ali, A. E. Hasan, and T. S. Abu-Zaid, “A field study on replacing traditional flood irrigation of sugarcane crop in upper Egypt with drip irrigation technique,” *Appl. Water Sci.*, vol. 15, no. 8, pp. 1–21, 2025, doi: 10.1007/s13201-025-02554-7.

[3] L. Rodrigo and I. Munaweera, “Employing sustainable agriculture practices using eco-friendly and advanced hydrogels,” *RSC Adv.*, vol. 15, no. 26, pp. 21212–21228, 2025, doi: 10.1039/d5ra03035h.

[4] L. Valgimigli, “Lipid Peroxidation and Antioxidant Protection,” *Biomolecules*, vol. 13, no. 9, 2023, doi: 10.3390/biom13091291.

[5] N. Illouz-Eliaz *et al.*, “Drought recovery in plants triggers a cell-state-specific immune activation,” *Nat. Commun.* , vol. 16, no. 1, 2025, doi: 10.1038/s41467-025-63467-2.

[6] N. Pettinelli *et al.*, “Sodium alginate-g-polyacrylamide hydrogel for water retention and plant growth promotion in water-deficient soils,” *Ind. Crops Prod.*, vol. 222, no. September, 2024, doi: 10.1016/j.indcrop.2024.119759.

[7] V. Prashar, M. Nandal, R. K. Gupta, and Y. K. Tyagi, “Novel Synthesis, and Application of Carboxymethylated Cassia fistula-Based Hydrogel for Extended-Release of Dinotefuran,” *ChemistrySelect*, vol. 9, no. 46, pp. 1–12, 2024, doi: 10.1002/slct.202403421.

[8] A. Roy *et al.*, “Review Article Role of Microbes and Nanomaterials in the Removal of Pesticides from Wastewater,” vol. 2022, 2022, doi: 10.1155/2022/2131583.

[9] C. Tian *et al.*, "Effects of a controlled-release fertilizer on yield, nutrient uptake, and fertilizer usage efficiency in early ripening rapeseed (Brassica napus L.)," *J. Zhejiang Univ. Sci. B*, vol. 17, no. 10, pp. 775–786, 2016, doi: 10.1631/jzus.B1500216.

[10] S. Luo, Y. Liu, F. Jiang, Y. Liang, G. Huang, and B. Lin, "Biosafe alginate-based dual-pesticides controlled release system for selective control of multiple pests," *Chem. Eng. J.*, vol. 518, no. April, p. 164703, 2025, doi: 10.1016/j.cej.2025.164703.

[11] V. Hasija, K. Sharma, V. Kumar, S. Sharma, and V. Sharma, "Green synthesis of agar / Gum Arabic based superabsorbent as an alternative for irrigation in agriculture," *Vacuum*, vol. 157, no. July, pp. 458–464, 2018, doi: 10.1016/j.vacuum.2018.09.012.

[12] K. Farooq *et al.*, "Synthesis and characterization of biodegradable AL-g-poly(AAM) hydrogel-based novel matrix for slow and controlled root-targeted delivery of fertilizers," *J. Polym. Res.*, vol. 32, no. 3, pp. 1–18, 2025, doi: 10.1007/s10965-025-04304-4.

[13] H. Cao, L. Duan, Y. Zhang, J. Cao, and K. Zhang, "Current hydrogel advances in physicochemical and biological response-driven biomedical application diversity," *Signal Transduct. Target. Ther.*, vol. 6, no. 1, pp. 1–31, 2021, doi: 10.1038/s41392-021-00830-x.

[14] L. T. Mashabela *et al.*, "A Comprehensive Review of Cross-Linked Gels as Vehicles for Drug Delivery to Treat Central Nervous System Disorders," *Gels*, vol. 8, no. 9, 2022, doi: 10.3390/gels8090563.

[15] G. H. D. Agbna and S. J. Zaidi, "Hydrogel Performance in Boosting Plant Resilience to Water Stress—A Review," *Gels*, vol. 11, no. 4, 2025, doi: 10.3390/gels11040276.

[16] E. Verni *et al.*, "Development and characterization of novel tannin-modified konjac glucomannan hydrogels with optimized crosslinking features,"

Carbohydr. Polym. Technol. Appl., vol. 11, no. March, p. 100875, 2025, doi: 10.1016/j.carpta.2025.100875.

[17] M. Kumari *et al.*, "Acacia catechu (L.f.) Willd.: A Review on Bioactive Compounds and Their Health Promoting Functionalities," *Plants*, vol. 11, pp. 1–19, 2022.

[18] A. Duval and L. Avérous, "Characterization and Physicochemical Properties of Condensed Tannins from Acacia catechu," *J. Agric. Food Chem.*, vol. 64, no. 8, pp. 1751–1760, Mar. 2016, doi: 10.1021/acs.jafc.5b05671.

[19] A. Koopmann, C. Schuster, and J. Torres-rodr, "Tannin-Based Hybrid Materials and Their," pp. 1–32.

[20] K. Yamauchi, M. Soyano, M. Kobayashi, and Y. O. Kamatari, "Protein aggregation model to explain the bioactivity of condensed tannins," *Food Chem.*, vol. 416, no. July 2022, p. 135870, 2023, doi: 10.1016/j.foodchem.2023.135870.

[21] Y. Wu *et al.*, "Advances in gum-based hydrogels and their environmental applications," *Carbohydr. Polym.*, vol. 318, no. December 2022, p. 121102, 2023, doi: 10.1016/j.carbpol.2023.121102.

[22] V. Prashar and R. K. Gupta, "A Review of Natural Gums and Mucilage-Based Hydrogels for Food , Agriculture , Biomedical , and Cosmetics," pp. 1–38, 2026, doi: 10.1002/tcr.202500238.

[23] M. Kamran, A. ul H. A. Shah, G. Rahman, and S. Bilal, "Potential Impacts of Prunus domestica Based Natural Gum on Physicochemical Properties of Polyaniline for Corrosion Inhibition of Mild and Stainless Steel," *Polymers (Basel).*, vol. 14, no. 15, 2022, doi: 10.3390/polym14153116.

[24] A. Sharma, P. R. Bhushette, and U. S. Annapure, "Purification and physicochemical characterization of Prunus domestica exudate gum polysaccharide," *Carbohydr. Polym. Technol. Appl.*, vol. 1, no. September, p.

100003, 2020, doi: 10.1016/j.carpta.2020.100003.

[25] P. Feng *et al.*, "An eco-friendly MIL-101@CMCS double-coated dinotefuran for long-acting active release and sustainable pest control," *J. Clean. Prod.*, vol. 265, p. 121851, 2020, doi: 10.1016/j.jclepro.2020.121851.

[26] S. Zhao *et al.*, "Exploring the Impact of Dinotefuran Residue on Microbial Community and Flavor Generation in Huangjiu Fermentation," 2025, doi: 10.1021/acs.jafc.5c02308.

[27] J. Zhang *et al.*, "Ecotoxicological effects of the neonicotinoid insecticide dinotefuran on springtails (Folsomia candida) at soil residual concentration," *Pestic. Biochem. Physiol.*, vol. 209, no. December 2024, p. 106345, 2025, doi: 10.1016/j.pestbp.2025.106345.

[28] J. Li *et al.*, "An occupational health assessment of dinotefuran exposure in greenhouse vegetable workers : Metabolomic profiling and toxicokinetic analysis," vol. 491, no. December 2024, 2025.

[29] M. Nandal, D. Kumar, and R. K. Gupta, "Harnessing Lignite-Based Hydrogel for Enhanced UV Protection and Delivery of Dinotefuran in Agriculture," *ChemistrySelect*, vol. 10, no. 25, pp. 1–13, 2025, doi: 10.1002/slct.202405884.

[30] T. Jamnongkan and S. Kaewpirom, "Potassium Release Kinetics and Water Retention of Controlled-Release Fertilizers Based on Chitosan Hydrogels," pp. 413–421, 2010, doi: 10.1007/s10924-010-0228-6.

[31] A. Singh, A. K. Kar, D. Singh, R. Verma, and N. Shraogi, "composite hydrogel beads as carrier for controlled release of Imidacloprid towards sustainable pest control," vol. 427, no. June 2021, 2022.

[32] M. A. Shaheed, M. Nandal, D. Kumar, and R. K. Gupta, "A novel Iraqi Prunus Domestica gum and lignin as natural precursors for the development of hydrogels for the slow release of thiamethoxam," vol. 33, no. March, pp. 149–169, 2026, doi: 10.56042/ijct.v33i2.25734.

[33] S. G. Warkar and A. Kumar, “Synthesis and assessment of carboxymethyl tamarind kernel gum based novel superabsorbent hydrogels for agricultural applications,” *Polymer (Guildf).*, vol. 182, no. September, p. 121823, 2019, doi: 10.1016/j.polymer.2019.121823.

[34] Z. Shi *et al.*, “International Journal of Biological Macromolecules Synthesis and characterization of porous tree gum grafted copolymer derived from Prunus cerasifera gum polysaccharide,” *Int. J. Biol. Macromol.*, vol. 133, pp. 964–970, 2019, doi: 10.1016/j.ijbiomac.2019.04.128.

[35] B. Ni, M. Liu, and S. Lü, “Multifunctional slow-release urea fertilizer from ethylcellulose and superabsorbent coated formulations,” vol. 155, pp. 892–898, 2009, doi: 10.1016/j.cej.2009.08.025.

[36] W. Zhang, X. Mu, Y. Xu, G. Ma, and Z. Lei, “Research progress of environment-responsive hydrogel,” *Express Polym. Lett.*, vol. 18, no. 2, pp. 193–213, 2024.

[37] A. Bora and N. Karak, “Starch and itaconic acid-based superabsorbent hydrogels for agricultural application,” *Eur. Polym. J.*, vol. 176, no. July, p. 111430, 2022, doi: 10.1016/j.eurpolymj.2022.111430.

[38] S. Noureen *et al.*, “European Journal of Pharmaceutical Sciences A novel pH-responsive hydrogel system based on Prunus armeniaca gum and acrylic acid : Preparation and evaluation as a potential candidate for controlled drug delivery,” *Eur. J. Pharm. Sci.*, vol. 189, no. May, p. 106555, 2023, doi: 10.1016/j.ejps.2023.106555.

[39] M. Nandal, V. Prashar, M. Bansiwal, I. Kapoor, T. Kansal, and R. K. Gupta, “Novel molasses-grafted poly(sodium acrylate) hydrogel: A sustainable solution for water retention and controlled dinotefuran release,” *Indian J. Chem. Technol.*, vol. 32, no. 2, pp. 161–175, 2025, doi: 10.56042/ijct.v32i2.15397.

[40] S. Sethi, S. Balbir, S. Kaith, M. Kaur, and N. Sharma, “Cross-linked xanthan

gum – starch hydrogels as promising materials for controlled drug delivery," *Cellulose*, vol. 27, no. 8, pp. 4565–4589, 2020, doi: 10.1007/s10570-020-03082-0.

[41] M. Rizwan *et al.*, "pH Sensitive Hydrogels in Drug Delivery : Brief History , Properties , Swelling , and Release Mechanism , Material Selection and Applications", doi: 10.3390/polym9040137.

[42] M. P. Patil and N. J. Gaikwad, "Characterization of gliclazide-polyethylene glycol solid dispersion and its effect on dissolution," vol. 47, 2011.

[43] U. V Deore and H. S. Mahajan, "Isolation and structural characterization of mucilaginous polysaccharides obtained from the seeds of Cassia uniflora for industrial application," *Food Chem.*, vol. 351, no. January, p. 129262, 2021, doi: 10.1016/j.foodchem.2021.129262.

[44] S. S. Banerjee and D. Chen, "Fast removal of copper ions by gum arabic modified magnetic nano-adsorbent," vol. 147, pp. 792–799, 2007, doi: 10.1016/j.jhazmat.2007.01.079.

[45] L. Shi, W. Liu, X. Zhang, and J. Hu, "Preparation of Lignin Sulfonate Based / Organo - Montmorillonite Composite Hydrogel for Adsorbing Methylene Blue from Aqueous Solution," *J. Polym. Environ.*, vol. 30, no. 10, pp. 4287–4303, 2022, doi: 10.1007/s10924-022-02508-z.

[46] S. Uluata, "International Journal of Biological Macromolecules Malatya apricot gum : A source of natural gum and its physicochemical , functional and antioxidant properties," vol. 301, no. January, 2025.

[47] M. Worzakowska, "Thermal behavior , decomposition mechanism and some physicochemical properties of starch-g-poly (benzyl acrylate) copolymers," *J. Therm. Anal. Calorim.*, vol. 126, no. 2, pp. 531–540, 2016, doi: 10.1007/s10973-016-5603-7.

[48] B. Singh and V. Sharma, "Influence of polymer network parameters of

tragacanth gum-based pH responsive hydrogels on drug delivery," vol. 101, pp. 928–940, 2014.

[49] D. Balodhi, S. G. Warkar, A. Rani, and R. K. Gupta, "Natural carbohydrate gums based hydrogels," vol. 28, no. May, pp. 262–273, 2021.

[50] B. Singh, M. Mohan, and R. Kumar, "Food Hydrocolloids for Health Synthesis of hydrocortisone containing dietary fiber almond gum-based hydrogels as sustained drug delivery carriers for use in colon inflammation," *Food Hydrocoll. Heal.*, vol. 2, no. February, p. 100057, 2022, doi: 10.1016/j.fhfh.2022.100057.

[51] R. K. Gupta and D. Kumar, "Synthesis , characterization and application of Lignosulphonate-g- poly (sodium acrylate) hydrogel," vol. 30, no. November, pp. 753–764, 2023, doi: 10.56042/ijct.v30i6.1325.

[52] I. S. Raja and N. N. Fathima, "Porosity and dielectric properties as tools to predict drug release trends from hydrogels," pp. 1–10, 2014.

[53] N. Thombare, S. Mishra, M. Z. Siddiqui, U. Jha, D. Singh, and G. R. Mahajan, "Design and development of guar gum based novel , superabsorbent and moisture retaining hydrogels for agricultural applications," *Carbohydr. Polym.*, vol. 185, no. January, pp. 169–178, 2018, doi: 10.1016/j.carbpol.2018.01.018.

[54] C. R. Study, "New Organomineral Complex from Humic Substances Extracted from Poultry Wastes: Synthesis, Characterization and Controlled Release Study," vol. 29, no. 1, pp. 140–150, 2018.

[55] D. E. Ciolacu, R. Nicu, and F. Ciolacu, "Cellulose-Based Hydrogels as Sustained Drug-Delivery Systems," *Materials (Basel).*, vol. 13, no. 22, p. 5270, Nov. 2020, doi: 10.3390/ma13225270.

[56] S. Z. Tapdiqov and D. B. Taghiyev, "Application of kinetic results of doxorubicin release from polyacrylic acid-based hydrogel to Higuchi,

Korsmeyer-Peppas, Hixon-Crowell equations," *SOCAR Proc.*, vol. d, no. 1, pp. 130–135, 2025, doi: 10.5510/OGP20250101052.

[57] L. M. Nguyen *et al.*, "Materials Advances for controlled drug release : characterization , kinetic modeling , and in vitro evaluation," no. i, pp. 7574–7584, 2025, doi: 10.1039/d5ma00645g.

[58] K. Nandal, V. Vaid, P. Saini, and R. Kumar, "Industrial Crops & Products Synthesis and characterization of κ -carrageenan and guar gum-based hydrogels for controlled release fertilizers : Optimization , release kinetics , and agricultural impact," *Ind. Crop. Prod.*, vol. 225, no. December 2024, p. 120587, 2025, doi: 10.1016/j.indcrop.2025.120587.

[59] M. S. Lobo and P. Costa, "Modeling and comparison of dissolution profiles ´," vol. 13, pp. 123–133, 2001.

[60] U. Leków and Z. H. Ż. Eli, "DRUG RELEASE FROM HYDROGEL MATRICES," vol. 17, no. 2, 2010.